



## DETAILED FLOW VISUALIZATION AROUND COMPLEX BODIES

A. Yamamoto<sup>1</sup>, D. Nakamura<sup>2</sup>, S. Mizuki<sup>3</sup>, and H. Tsujita<sup>3</sup>

**Keywords:** 3D measurements, airplane, sports car, graphic representation, streamlines, visualization, secondary flow, external flow, pressure loss, Pitot tube, laboratory automation

### ABSTRACT

*Flows around geometrically complex bodies, such as whole airplane models and sports car models, have been measured in a small wind tunnel especially designed for detailed and precise measurements with a full-automatic controlled traverse gear. Lots of data were obtained using a micro five-hole Pitot tube to make clear the flow mechanisms around the bodies with help of computer graphic software for three-dimensional flow analyses. Pressure and velocity fields were visualised in the three dimensional space, vortex and even separated/reverse flow regions were detected from the resultant visualisation pictures. The present technique gives 'quantitative' visualisation of the flows around complex bodies and enables us to make 'invisible' quantities clearly visible. Three-dimensional streamlines or particle paths were also obtained from experimental data.*

### 1 INTRODUCTION

For airplanes and cars, for example, it is important to know behaviors of the external flows around the complete bodies in order to improve the aerodynamic performance with decreasing the fluid drag of such geometrically complex bodies. For estimating the performance qualitatively and quantitatively, wind tunnels are often used with reduced scale models. In the present paper, a detailed quantitative flow visualization technique is demonstrated for external flows around complex bodies. Very precise measurements are needed for this purpose with an automatic-controlled measuring device. Lots of measuring points are distributed on such fine grids as used in CFD analyses around the test bodies. In certain cases, the measuring fields need to be divided into several multi-block regions as used in CFD work. The quantitative data can be visualized using advanced graphic software often used in CFD post analyses. Similar techniques have already been applied to the internal flows of turbine cascades successfully by the author's group since 1985 [1,2] and to external flows of airplanes in 1995 [3]. But the recent advanced technologies in measuring techniques and in computer graphic software have made this quantitative flow visualization (QFV) more attractive and easier than before. The present study was done as his graduate study of one of the authors (D. Nakamura) at the National Aerospace Laboratory in 1999 [4].

**Authors:** <sup>1</sup>Aeroengine Research Division, National Aerospace Laboratory, Chofu-shi, Tokyo  
<sup>2</sup>Tochigi R&D Center, Honda R&D, Co., Ltd., Haga-gun, Tochigi  
<sup>3</sup>Department of Mechanical Engineering, Hosei University, Musashino-shi, Tokyo

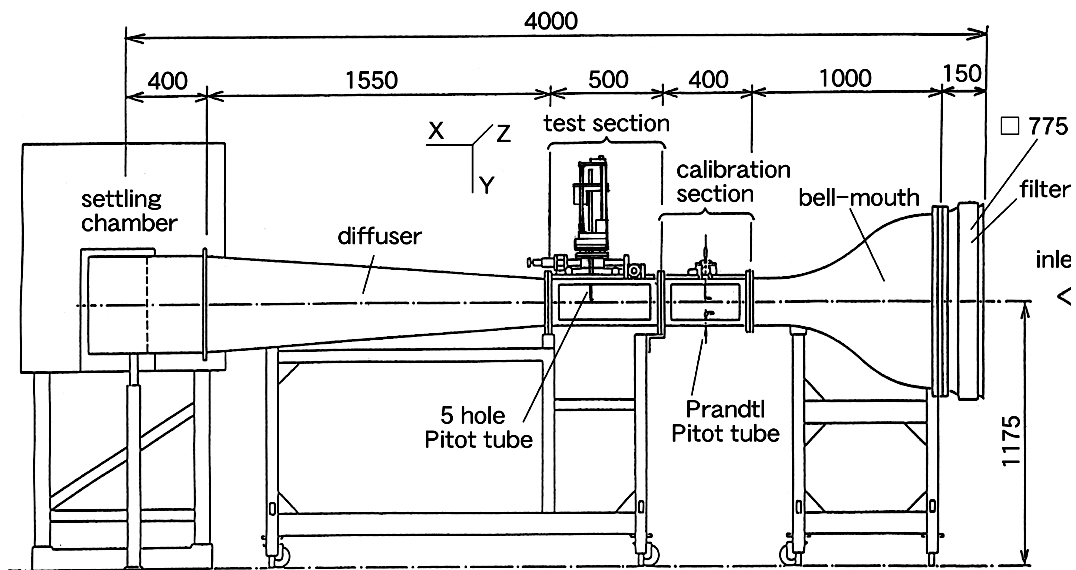


Fig. 1. The small wind tunnel

## 2 EXPERIMENTAL AND ANALYSIS METHODS

### 2.1 The test rig

The wind tunnel used in the present study is shown in Fig.1. The tunnel is of a suction type; air is swallowed from the atmosphere through the bell-mouth, contracted to one fifteenth time in the contraction chamber, and then led to the test section. After the test section, the air passes a diffuser duct, a settling chamber for being settled and for noise reduction and finally, is exhausted to the atmosphere again. The test section is of a rectangular duct which dimensions are 500mm in the axial (x) or flow direction, 140mm in the horizontal (z) direction and 200mm in the vertical (y) direction. On the upper wall of the test section, an automatic control traverse gear is installed to move a micro five-hole Pitot tube in three directions.

### 2.2 The experimental and analysis methods

Fig.2 shows flow paths of measured data and control signals of the traverse gear in the present measuring system. A five-hole Pitot tube has the head size of 1.5mm and is moved by the traverse gear combined with a programmable motor controller and a PC (measuring

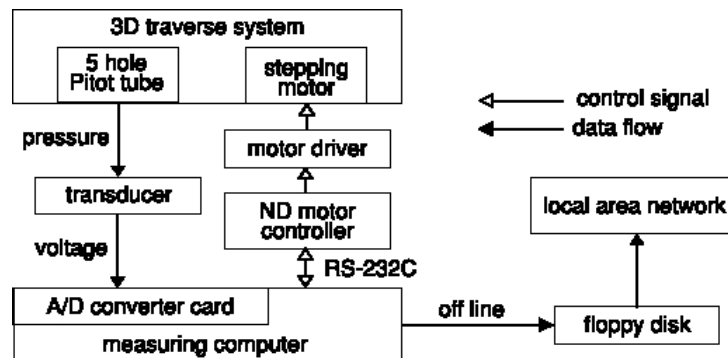


Fig.2. Flow chart of measured data and control signals

## DETAILED FLOW VISUALIZATION AROUND GEOMETRICALLY COMPLEX BODIES



**Fig. 3. Test models: B747-400 with winglet (upper left), B747-300 without winglet (upper right), F310B (lower)**

computer) to arbitrary points around the test model. Pressure data of the Pitot tube was taken in and converted by five individual pressure transducers into analog electric voltages and then taken into the PC through a multi-channel A/D converter. A vast number of data stored in the PC was then transferred to another computer through LAN for analyses and to visualize using three-dimensional graphic software such as TECPLOT. Test models used in the present study include two types of minutia airplane models, Boeing B747-300 (without winglet) and B747-400 (with winglet and a little longer wing span than -300) and a minutia sports car model, Ferrari F310B. All are shown in Fig.3. The sizes of the two airplane models are 1/500 of the actual sizes and that of the car model is of 1/18. The flow velocity at the inlet of the test section was kept constant at 40m/s during the present study. The corresponding Reynolds numbers were about  $4.3 \cdot 10^5$  for the airplanes and  $3 \cdot 10^5$  for the car, both defined by using the lateral widths of the models and the inlet velocity. Note that such minutia models are for demonstration purpose only of the present technique and a large discrepancy in Reynolds numbers between the present tests and the actual operations exists. This discrepancy should be taken into consideration, of course, when the results are interpreted in detail. The winglet means a small tip wing installed at the tip of the main wings and is fold upward as seen in Fig.3. Effects of the winglet on the flow quantities such as velocity, pressure loss, vortex formation, etc. around the airplanes will be discussed. Effects of so-called ‘angle of attack’ of the upstream flow of the airplanes will also be discussed. The angles tested were 0 and +5deg. In the following discussion, secondary flow or vector means projected velocity component of the resultant velocity onto the y-z plane that is normal to the axis of the wind tunnel (see Fig.1 for the coordinate definition). Loss means total pressure loss caused by the test body, and its dimensionless form was obtained by normalizing the loss by the inlet dynamic pressure, i.e.,  $(P_{t, \text{before}} - P_{t, \text{after}}) / (0.5 \cdot \rho \cdot V_{\text{in}}^2)$ , where  $\rho$  is density and  $V_{\text{in}}$  is the inlet velocity (40m/s).

### 3 RESULTS AND DISCUSSION

#### 3.1 Flow fields just behind B747-300 and -400 at two angles of attack, 0 and +5deg

Flows just downstream of the main wing are shown in Fig.4 for the two types of airplanes with/without winglet and for two angles of attack, 0 and +5deg. In this case, measurements were made in the region extending from about 20mm upstream from the trailing edge of the main wing tip to about +86mm from downstream of the airplane tail with uniform axial measuring interval of 2mm. Here, only some example pictures obtained at one measuring plane located at about 3mm just behind the main wing of each test airplane are presented to see secondary flows and the associated total pressure losses. These pictures show the flows being looked from the downstream side. The airplane body is located outside of the right-hand edge of each picture. Red colour shows higher loss while blue colour shows lower loss. Tracing the secondary flow vectors also draws some vortex lines.

In any of the figures, three loss cores (high loss areas) are seen, i.e., one behind the wing tip and two behind the two engines installed on the main wing. Vortices around each loss core are rotating in the same clockwise direction. At angle of attack +5deg, these vortices are more clearly seen and are stronger with bigger loss cores than at 0deg. Around the whole main wing, a large clockwise circulation is also seen. This circulation would easily be induced around the present type of swept wing. This circulation is clearer at angle of attack +5deg than 0deg.

As known well, lift of the airplane wing is generated from higher flow velocity (lower static pressure) over the upper surface of the wing and

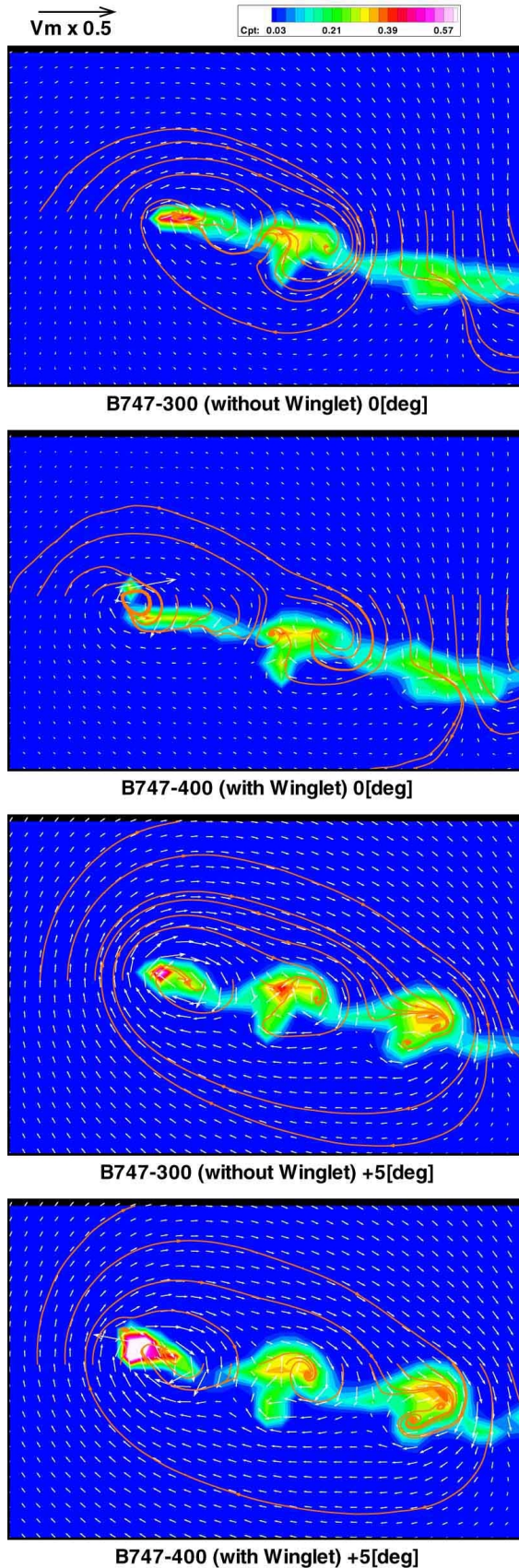


**Fig. 4. Loss coefficient and secondary flow vectors just behind the main wings of B747-300 and -400 at two angles of attack, 0 and +5deg**

## DETAILED FLOW VISUALIZATION AROUND GEOMETRICALLY COMPLEX BODIES

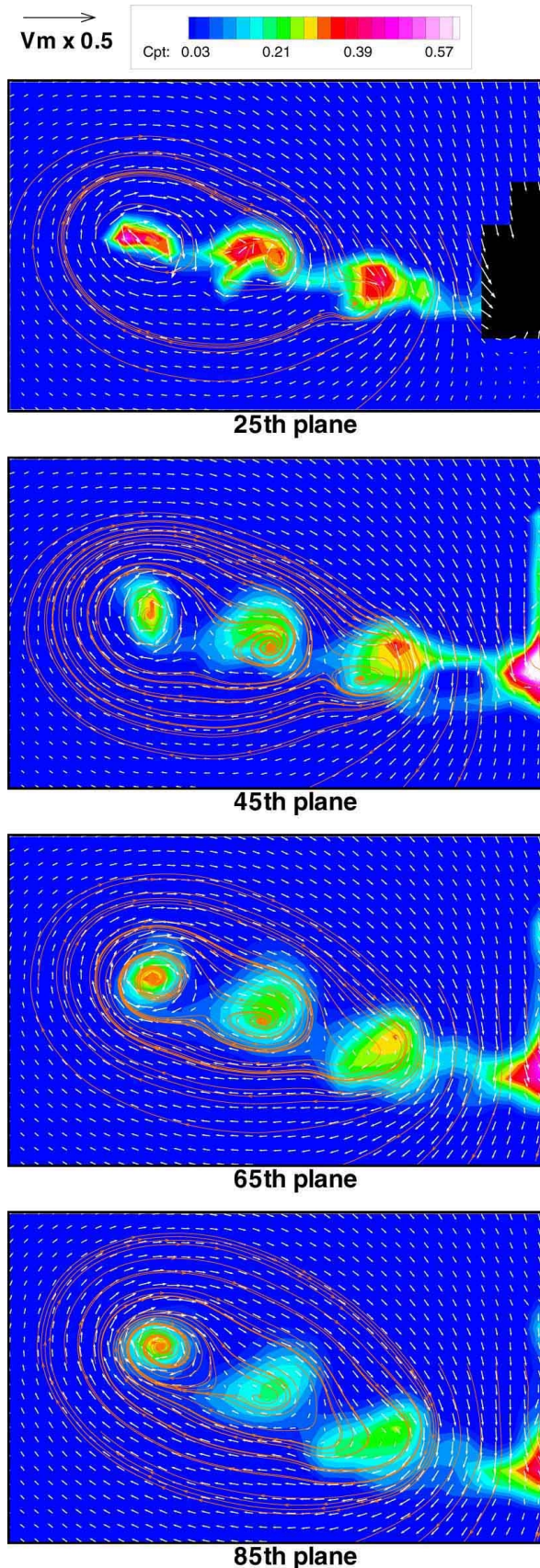


Fig. 5. Variation of Loss coefficient and secondary flow vectors downstream of the main wing of B747-300 without winglet at angle of attack +5deg

the lower flow velocity (higher static pressure) below the lower surface. The flow near the wing tip tends to move toward the upper side from the lower side due to the resultant pressure gradient. This would cause a downward induced velocity onto the upper surface of the wing to reduce the lift. A purpose of the winglet is to diffuse the tip vortex in order to reduce the induced downward velocity. This effect of the winglet can be seen from the comparison between the upper two figures in Fig.4 without and with winglet where downward velocity vectors near the wing tip are significantly reduced in the case with winglet compared to the case without winglet, at angle of attack 0deg. Also the tip loss is reduced. Comparison between the lower two figures in Fig.4 without and with winglet at angle of attack +5deg, however, does not show this effect so significantly. The losses and the vortices are nearly similar in both cases and therefore, the merit of the winglet can not be recognized. The wing tip loss is rather increased for the case with winglet. In the domestic flights like in Japan with short flight distance, most B747-400 airplanes are not installed winglets. This would be probably from the above reason that the winglet installation would not be so attractive for domestic flights that need often take-off and landing as for international flights with long horizontal flight distance.

### 3.2 Variation of flow fields behind B747-300 at angle of attack +5deg

To see the flow variation in the axial direction behind B747-300 without winglet in detail, more detailed measurements were made. The measuring region was extended widely in the axial direction from 22mm from upstream of the main wing tip to 172mm from downstream of the airplane tail with the same uniform measuring

interval of 2mm as before. Fig.5 shows secondary flow vectors, some vortex lines, and total pressure losses at four selected planes, 25<sup>th</sup>, 45, 65 and 85<sup>th</sup> planes. The 25<sup>th</sup> plane is located at about 9mm downstream from the trailing edge of the main wing tip and the four planes are located separately from each other with 40mm axial interval. It can be seen that each loss is diffusing as the flow goes downstream from 25<sup>th</sup> to 85<sup>th</sup> plane; the peak value of each loss decreases and the area gets wider. In particular, the loss area of the wing tip vortex has a horizontally long shape at the beginning, then changes to a vertically long one and finally, becomes the circular shape. This tip vortex is strongest among the three and mainly promotes to cause a large single circulation around the whole wing as the vortex lines show. The circulation and the rotation of all three vortices are in the same clockwise direction. The whole wake itself is slowly rotating also in the clockwise direction around the center of the tip vortex that is nearly fixed at the same location. At 25<sup>th</sup> and 40<sup>th</sup> planes, both engine vortices can still be seen to exist and some of the vortex lines around these vortices are migrated into the corresponding vortex centers. At 65<sup>th</sup> plane, however, one engine vortex closer to the airplane body nearly disappears, and at 85<sup>th</sup> plane, another engine vortex too.

Fig.6 shows an overall picture of total pressure loss distributions around the B747-300 airplane. The loss distributions shown here correspond to those at a total of 17 planes starting from about 1mm to 129mm downstream of the wing tip with 8mm axial interval. Ten vortex lines are also plotted, starting from upstream of the wing tip. The picture clearly shows the three-dimensional flow field around the body. The streamlines are rolled up by the tip vortex as they go downstream. It is more clearly seen here than in the previous figures how the wakes are getting diffused around the body and how the streamlines and the wake itself rotate. In this figure, several multi-block regions we adopted in the present traverse measurements are also shown.

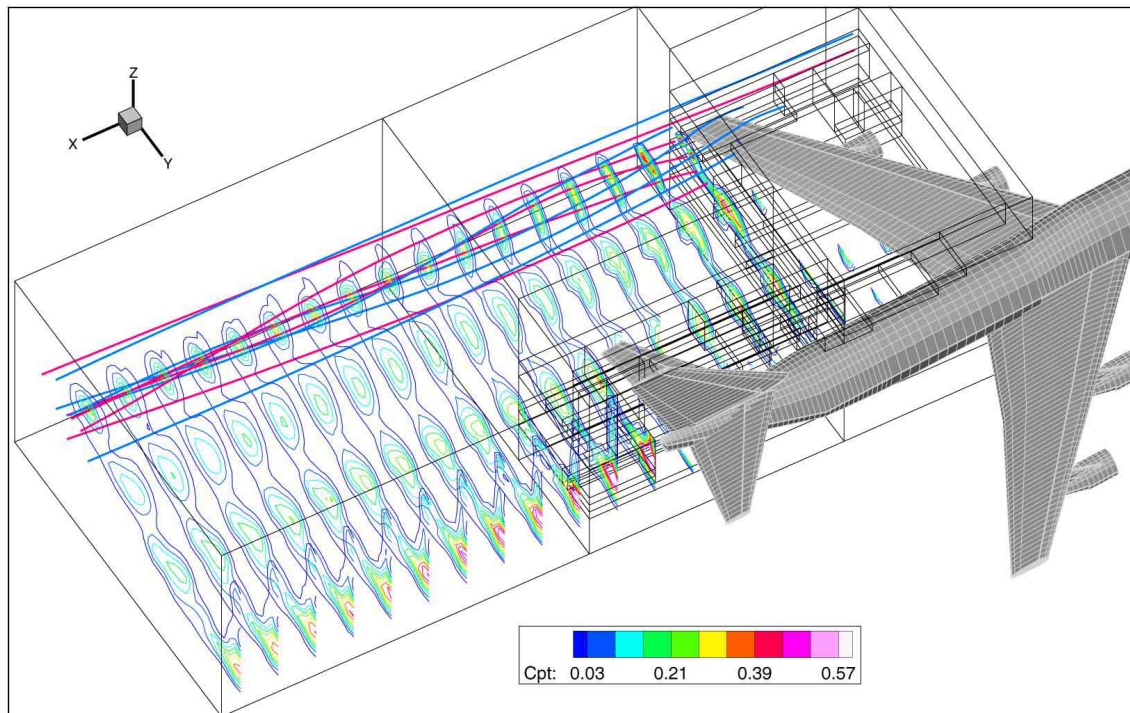


**Fig. 6. Loss coefficient around B747-300 and three-dimensional streamlines near the wing tip at angle of attack +5deg**

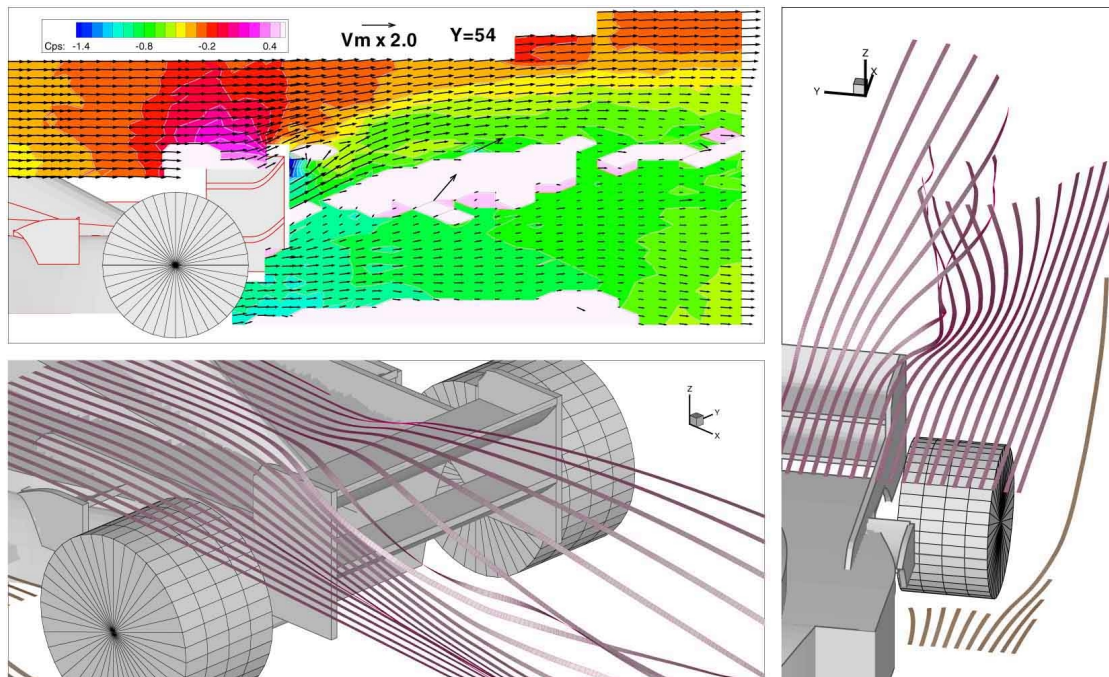


Fig. 7. Static pressure distribution (upper left) and three-dimensional streamlines (lower left and right) around a sports car

### 3.3 Flow visualization around a sports car

Flows around cars are considered to be much more complicated than the flows around airplanes; the flows might include large deflected upward or downward flows around the body, various vortices, separated and reverse flows caused by their more complicated shapes. In the present car model tested, for example, a rear wing is installed on the rear edge of the car, which may produce some complicated flows around it. In fact, the flows downstream of the car were very difficult to detect with the five-hole Pitot tube; a single survey of the flow was not enough and more complicated procedures were needed. To get meaningful data as much as possible in this kind of flow field with large deflected flows, several surveys at the same measuring region had to be repeated because of the limitation of the valid calibration angle range of the probe. From these surveys, only the meaningful data within the range was selected and used for analysis. The measuring region was extended in this test case from about 77mm upstream from the trailing edge of the rear wing to 111mm downstream of the same trailing edge. To save the very long measuring time required, the measuring planes were chosen with non-uniform axial intervals of 2 – 5mm.

Fig.7 shows some two- and three- dimensional representations of the flows around the rear part of the car. The upper left figure shows a static pressure distribution and resultant velocity vectors projected onto the vertical plane (two-dimensional x-z plane) which was located very close to the centerline of the car. Static pressure downstream of the car is very low and this indicates the drag of the car would be significant. The areas in white colour correspond to the regions where no data were available. Large deflected flows, unsteady flows, and reverse flows may exist in these areas. Vectors just over the two vanes of the rear wing indicate strongly deflected upward flows, like jet flows. The static pressure distribution just over the rear wing indicates a high-pressure region. Both the upward flows and the resultant high static pressure over the rear wing would produce downward forces on the car and make the car stable so as not to easily slip on the road.

Undetectable wakes are also recognized just downstream of each vane (small and large white areas).

The lower left and right figures in Fig.7 show two different views of the same three-dimensional streamlines obtained by tracing the resultant velocity vectors measured. As clearly seen here, some of the streamlines outside of the rear wing are deflected downward when they pass the endplate of the rear wing. This deflection is caused by the pressure/velocity gradient distributed around the rear wing region where the pressure is lower at the outer side of the endplate. The deflected flow would finally form a vortex rotating in the counter-clockwise direction when it is looked from the downstream side, and would produce losses. As seen here, the rear wing of the model car really works to decrease the lift that acts the car, oppositely to the airplane wing.

#### 4 CONCLUSIONS

- 1) A 'quantitative' flow visualisation (QFV) technique for external flows has been established with a novel fully automatic measuring system to get detailed experimental data and recent advanced three-dimensional graphic software to visualize the data.
- 2) The technique has then been applied to the external flows around three types of complex bodies such as two types of airplanes and one sports car. The results demonstrate the abilities to make 'invisible' quantities very clearly visible and to present the complex flow mechanisms quantitatively in easily understandable ways.

#### REFERENCES

- [1] Yamamoto, A., Quantitative Flow Visualization of Three-dimensional Flows in Turbine Cascades, Osaka Joint Meeting of FVSJ, Oct. 1985 (in Japanese).
- [2] Yamamoto, A., Internal Flow Analysis by Wind Tunnels and Its Graphic Representation, Symposium on Computer Contributions to Internal Flow Analyses of FVSJ, Nov. 1986 (in Japanese).
- [3] Inoue, S., Yamamoto, A., and Usui, H., Quantitative Flow Visualization around Airplanes, Kagoshima Meeting of VSJ. Oct. 1995 (in Japanese).
- [4] Nakamura, D., Study of Three Dimensional Quantitative Flow Visualization around Complex Geometries, Master Theses, Hosei University, Feb. 1999 (in Japanese).